A new robust regime for a dispersion-managed multichannel 2R regenerator

Taras I. Lakoba[1*] **and Michael Vasilyev**[2]

[1]*Department of Mathematics and Statistics, University of Vermont, Burlington, VT 05401*
[2]*Department of Electrical Engineering, University of Texas at Arlington, Arlington, TX 76019*
[*]*Corresponding author: lakobati@cems.uvm.edu*

Abstract: We study the performance of a multichannel version [M. Vasilyev and T.I. Lakoba, Opt. Lett. **30**, 1458 (2005)] of the all-optical Mamyshev regenerator in a practically important situation where one of its key components - a periodic-group-delay device - has a realistic amplitude characteristic of a bandpass filter. We show that in this case, the regenerator can no longer operate in the regime reported in our original paper. Instead, we have found a new regime in which the regenerator's performance is robust not only to such filtering, but also to considerable variations of regenerator parameters. In this regime, the average dispersion of the regenerator must be (relatively) large and anomalous, in constrast to what was considered in all earlier studies of such (single-channel) regenerators based on spectral broadening followed by off-center filtering. In addition, hardware implementation of a regenerator in the new regime is somewhat simpler than that in the original regime.

OCIS codes: (060.2330) Fiber optics communications; (060.4510) Optical communications; (060.5530) Pulse propagation and solitons; (070.4340) Nonlinear optical signal processing; (230.1150) All-optical devices; (230.4320) Nonlinear optical devices.

References and links

1. P. V. Mamyshev, "All-optical regeneration based on self-phase modulation effect," in *Proceedings of the 24th European Conference on Optical Communications* (ECOC, Madrid, Spain, 1998), Vol. **1**, pp. 475–476.
2. Y. Su, G. Raybon, R.-J. Essiambre, and T.-H. Her, "All-optical 2R regeneration of 40-Gb/s signal impaired by intrachannel four-wave mixing," IEEE Photon. Technol. Lett. **15**, 350–352 (2003).
3. T.-H. Her, G. Raybon, and C. Headley, "Optimization of pulse regeneration at 40 Gb/s based on spectral filtering of self-phase modulation in fiber," IEEE Photon. Technol. Lett. **16**, 200–202 (2004).
4. M. Matsumoto, "Performance analysis and comparison of optical 3R regenerators utilizing self-phase modulation in fibers," J. Lightwave Technol. **22**, 1472–1482 (2004).
5. M. Vasilyev and T. I. Lakoba, "All-optical multichannel 2R regeneration in a fiber-based device," Opt. Lett. **30**, 1458–1460 (2005).
6. M. Eiselt, "Does spectrally periodic dispersion compensation reduce non-linear effects?" in *Proceedings of the 25th European Conference on Optical Communications* (ECOC, Nice, France, 1999), Vol. **1**, pp. 144–145.
7. G. Bellotti and S. Bigo, "Cross-phase modulation suppressor for multispan dispersion-managed WDM transmission," IEEE Photon. Technol. Lett. **12**, 726–728 (2000).
8. X. Wei, X. Liu, C. Xie, and L. F. Mollenauer, "Reduction of collision-induced timing jitter in dense wavelength-division multiplexing by the use of periodic-group-delay dispersion compensators," Opt. Lett. **28**, 983–985 (2003).
9. L. F. Mollenauer, A. Grant, X. Liu, X. Wei, C. Xie, and I. Kang, "Experimental test of dense wavelength-division multiplexing using novel, periofic-group-delay-complemented dispersion compensation and dispersion-managed solitons," Opt. Lett. **28**, 2043–2045 (2003).

---

10. T. Ohara, H. Takara, A. Hirano, K. Mori, and S. Kawanishi, "40-Gb/s × 4-channel all-optical multichannel limiter utilizing spectrally filtered optical solitons," IEEE Photon. Technol. Lett. **15**, 763–765 (2003).

11. D. Yang, C. Lin, W. Chen, and G. Barbarossa, "Fiber Dispersion and Dispersion Slope Compensation in a 40-Channel 10-Gb/s 3200-km Transmission Experiment Using Cascaded Single-Cavity GiresTournois Etalons," IEEE Photon. Technol. Lett. **16**, 299–301 (2004).

12. W. Zhu, G. Barbarossa, D. Yang, and C. Lin, "Simulation and Design for a Tunable Dispersion Compensator Package," IEEE Trans. Compon. Packag. Technol. **27**, 513–522 (2004).

13. R. L. Lachance, S. Lelievre, and Y. Painchaud, "50 and 100 GHz multi-channel tunable chromatic dispersion slope compensator," in *Optical Fiber Communications Conference*, 2003 OSA Technical Digest Series (Optical Society of America, 2003), Vol. **1**, pp. 164–165.

14. L. M. Lunardi, D. J. Moss, S. Chandrasekhar, L. L. Buhl, M. Lamont, S. McLaughlin, G. Randall, P. Colbourne, S. Kiran, and C. A. Hulse, "Tunable Dispersion Compensation at 40 Gb/s using a multicavity etalon all-pass filter, with NRZ, RZ and CSRZ Modulation," J. Lightwave Technol. **20**, 2136–2144 (2002).

15. D. J. Moss, M. Lamont, S. McLaughlin, G. Randall, P. Colbourne, S. Kiran, and C. A. Hulse, "Tunable Dispersion and Dispersion Slope Compensators for 10 Gb/s Using All-Pass Multicavity Etalons," IEEE Photon. Technol. Lett. **15**, 730–732 (2003).

16. T. N. Nguyen, M. Gay, L. Bramerie, T. Chartier, and J.-C. Simon, "Noise reduction in 2R-regeneration technique utilizing self-phase modulation and filtering," Opt. Express **14**, 1737–1747 (2006).

17. A. Bertson, N.J. Doran, W. Forrysiak, and J.H.B. Nijhof, "Power dependence of dispersion-managed solitons for anomalous, zero, and normal path-average dispersion," Opt. Lett. **23**, 900–902 (1998).

18. M. Vasilyev and T. I. Lakoba, "Fiber-Based All-Optical 2R Regeneration of Multiple WDM Channels," in *Optical Fiber Communication Conference*, 2005 OSA Technical Digest on CD-ROM (Optical Society of America, 2005), paper OME62.

19. In this work, unlike in our earlier paper [5], we do not consider the 40 Gb/s case. For general scaling rules of regenerator parameters with the bit rate, we refer the reader to [5], where we also analyze the impact of higher spectral efficiency (at 40 Gb/s) on the regenerator performance. The focus of the present work is on studying the regenerator's performance for the parameters of a specific commercial PGDD available in the lab of the second author (M.V.) and designed for 10-Gb/s applications. At the moment, we do not have the information necessary to model a 40-Gb/s-compatible PGDD, without which information we could not proceed with a similar study of a multichannel regenerator at 40 Gb/s.

20. L. A. Provost, C. Finot, P. Petropoulos, K. Mukasa, and D. J. Richardson, "Design scaling rules for 2R-optical self-phase modulation-based regenerators," Opt. Express **15**, 5100–5113 (2007).

21. D. F. Grosz, A. Agarwal, S. Banerjee, D. N. Maywar, and A. P. Küng, "All-Raman ultralong-haul single-wideband DWDM transmission systems with OADM capability," J. Lightwave Technol. **22**, 423–432 (2004).

22. L. F. Mollenauer, S. G. Evangelides, and J. P. Gordon, "Wavelength division multiplexing with solitons in ultra-longdistance transmission using lumped amplifiers," J. Lightwave Technol. **9**, 362–367 (1991).

1. Introduction

All-optical regeneration is being actively researched as it can increase the reach of transmission systems without expensive optical-to-electrical signal conversion. Among various regeneration schemes, the one with 2R (re-amplification and re-shaping) capabilities proposed in [1] attracted particular attention due to its simplicity and robustness. In this regenerator, input pulses are first spectrally broadened by self-phase modulation after passing through a section of highly nonlinear fiber (HNLF). The regenerated pulses are sliced out of the broadened spectrum by an optical bandpass filter (OBPF) placed at the end of the HNLF, with the OBPF's central frequency being offset from the channel's center. Such a regenerator was shown (see, e.g., [1]–[4]) to reduce degradation of both the ZERO and ONE signal levels. However, a device with such attractive properties is still not considered as a practical alternative to electronic-domain regenerators because simultaneous regeneration of multiple wavelength-division multiplexing (WDM) channels presents a considerable challenge. Indeed, the strong nonlinear effects that enable the regeneration of a single channel lead to detrimental interchannel interactions and hence to signal distortion.

In a recent paper [5], we proposed a modification of the Mamyshev regenerator [1] to enable its handling of multiple WDM channels simultaneously. Our multichannel regenerator, whose schematics can be found in Fig. 1 of [5], employs a dispersion map where HNLF is divided into short sections, each followed by a periodic-group-delay device (PGDD). As in dispersion-

managed transmission systems, the dispersion map allows one to use high local dispersion to suppress nonlinear interchannel interactions while having relatively low average dispersion to maintain strong self-phase modulation. The PGDDs further suppress the detrimental interchannel interaction by ensuring a fast walk-off among pulses in different channels [6]–[9]. We numerically demonstrated that such a regenerator can improve the eye opening of a degraded signal by 1.2 dB for 10 Gb/s and by 0.9 dB for 40 Gb/s. In what follows we will refer to our modification [5] of the Mamyshev regenerator as a dispersion-managed (DM) regenerator to distinguish it from the originally proposed constant-dispersion (CD) Mamyshev regenerator [1]. It should be noted that a DM scheme employing alternating positive- and negative-dispersion fibers, but based on a different physical principle (that of soliton-like compression), was proposed for multichannel operation in [10]. However, due to the absence of PGDDs in that scheme, interchannel interactions were not suppressed sufficiently (even with the input power being less than what we use in the present paper), which necessitated polarization interleaving of adjacent channels and restricted the limiter of Ref. [10] to operate with only two pairs of co-polarized channels. In contrast, the multichannel regenerator proposed in [5] does not require any form of polarization control and is scalable to a large number of channels. Let us also note that our multichannel regenerator is expected to be cost-effective in a system employing sufficiently many channels. For systems employing only a few channels, the conventional single-channel opto-electronic repeaters may be a more cost-effective solution.

In a laboratory implementation of the DM regenerator [5], one needs to consider practical limitations of the currently available PGDDs. Apart from a 2–3 dB insertion loss, which can be mitigated by amplification, the known commercial (e.g. Avanex PowerShaper ^{TM} and Teraxion ClearSpectrum^{TM} tunable dispersion compensators) [11]–[13] and pre-commercial [14, 15] PGDDs have working bandwidths below 60% of their interchannel spacing. Beyond the working bandwidth, either the phase response becomes severely degraded, or considerable amplitude filtering occurs. Thus, an understanding of 2R regeneration in the presence of such amplitude filtering (typically, higher-order, or flat-top, Gaussian filter with 3-dB bandwidth smaller than 60% of channel spacing) is needed. In our original study [5], we pointed out that in certain cases, the presence of a rather wide and gentle (e.g., first-order Gaussian) amplitude characteristic in a PGDD may actually improve the performance of a multichannel regenerator. However, the amplitude characteristic of a commercially available PGDD is neither gentle nor wide in comparison with the interchannel spacing.

In our simulations presented below, we observe that the presence of such a charactristic significantly degrades the performance of a regenerator operated in the regime reported in [5]. (By a "regime", we mean both the strength of the dispersion map and the average dispersion in the device.) Therefore, we searched for an alternative regime that would guarantee good performance of the regenerator in the presence of the aforementioned amplitude characteristic of a PGDD. We found such a regime, which, furthermore, turns out to be more robust to variations of the regenerator parameters than the original regime reported in [5]. This is the main result of the present study.

It should be noted that the role of a filter at the input of the regenerator was previously studied in [16]. However, that study was concerned with the effect of filtering on the evolution of noise (amplitude spontaneous emission) in the regenerator. In our work, we do not consider noise. Rather, we study the effect of the bandpass filtering on the *shape* of the input-output power transfer function of the regenerator.

The main part of this paper is organized as follows. In Section 2 we present results for single-channel regenerators. They will guide us in selecting suitable parameters for multichannel operation, which is considered in Section 3. In both Sections 2 and 3, we neglected the losses of the PGDDs and the HNLF. This is done to have a direct comparison of our present results with

those of Ref. [5], which were also obtained for this lossless case. In Section 4, we demonstrate that the account of these losses, periodically compensated at few locations along the regenerator, does not qualitatively change the results of the previous sections. Namely, the shape of the power transfer curves is changed only slightly, while the eye opening improvement, brought in by the regenerator, is degraded by 0.1–0.4 dB compared to the lossless case, depending on the details of the loss-compensating scheme. Finally, in Section 5, we summarize conclusions of this work.

2. Single-channel results for the lossless case

The main outcome of single-channel simulations will be input-output power transfer curves, which will indicate the range of dispersion map parameters suitable for multichannel operation of the regenerator. These curves are obtained by numerically simulating the standard nonlinear Schrödinger equation, as explained in [5, 18]. In all the simulations reported below, the bit rate is 10 Gb/s [19] and input pulses are Gaussian-shaped with the full width at half maximum (FWHM) being $T_{\mathrm{FWHM}} = 33$ ps. The data modulator at the transmitter is assumed to have the electrical bandwidth of 12 GHz, and at the input of a regenerator, the pulses pass through a channel multiplexer that has the amplitude characteristic of a 3rd-order Gaussian with the optical bandwidth of 35 GHz at FWHM. The finite bandwidths of both the data modulator and the multiplexer result in a slight patterning effect whereby the input pulses have slightly different peak powers depending on whether they are adjacent to ZERO or ONE slots (see Fig. 1). At the output of the regenerator, the pulses first go through a demultiplexer whose amplitude characteristic coincides with that of the multiplexer and then pass through an optical bandpass filter (OBPF) whose center is offset from the center of the channel by 25 GHz. The OBPF is taken to be a 13.3-GHz-wide Gaussian to restore the original shape and width of the pulses. For the single-channel simulations, we use a bit sequence 0110101111001110 (see Fig. 1(b)), which contains all possible combinations of adjacent pulse patterns. The extinction ratio of these pulses is 35 dB (essentially infinite). All input pulses have nearly the same power (with the slight variations seen in Fig. 1 being due to the aforementioned patterning effect); we vary this input peak power between 20 and 320 mW to obtain input-output power transfer curves reported below.

The DM regenerator (for schematics, see Fig. 1 of [5]), consists of several identical cells, with each cell being composed of a section of a high-normal-dispersion HNLF followed by a PGDD. The role of the PGDDs is to (partially) compensate the dispersion of the HNLF *within each channel* and, at the same time, to ensure fast walk-off among pulses *in different channels*, which reduces detrimental interchannel interactions. The most obvious choice for the dispersive HNLF is the commercial dispersion-compensating fiber. Under this assumption, the nonlinearity parameter of the HNLF is 5 $(\mathrm{W \cdot km})^{-1}$ and the dispersion coefficient (except for one instance of a CD regenerator considered below) $D_{\mathrm{HNLF}} = -120$ ps/nm/km. The values of the average dispersion of the regenerator and the lengths L_{HNLF} and the number of HNLF sections will be reported below for each simulation separately. The average dispersion is defined as

$$D_{\mathrm{av}} = \frac{D_{\mathrm{HNLF}} L_{\mathrm{HNLF}} + \mathscr{D}_{\mathrm{PGDD}}}{L_{\mathrm{HNLF}}}, \tag{1}$$

where $\mathscr{D}_{\mathrm{PGDD}}$ is the accumulated dispersion of a PGDD. (Since the PGDD is considered as a linear device, only its accumulated dispersion rather than the dispersion coefficient and the length separately, is of physical significance.) For future reference, we also define the map strength similarly to how it is commonly done for DM solitons (see, e.g., [17]):

$$S \equiv \frac{\lambda^2}{2\pi c} \frac{|D_{\mathrm{HNLF}} L_{\mathrm{HNLF}} - \mathscr{D}_{\mathrm{PGDD}}|}{T_{\mathrm{FWHM}}^2} \approx \frac{\lambda^2}{2\pi c} \frac{2|D_{\mathrm{HNLF}} L_{\mathrm{HNLF}}|}{T_{\mathrm{FWHM}}^2}, \tag{2}$$
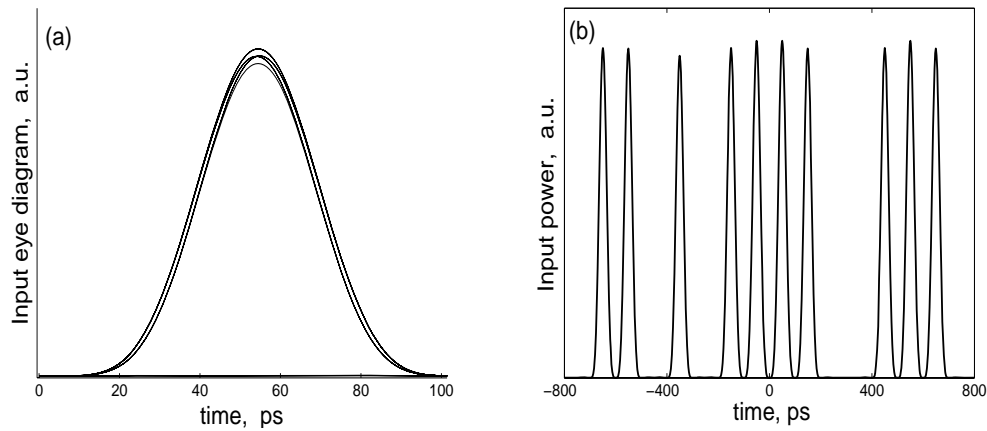
Fig. 1. Regenerator input for single-channel simulations.

where λ is the carrier wavelength (1580 nm in our simulations) and c is the light speed in vacuum. Thus, S is proportional to the ratio of L_{HNLF} to the dispersion length of the pulse in the (first) HNLF section. In DM-soliton-based transmission systems, which are *weakly* nonlinear, an increase of the map strength is known to lead to increased dispersive breathing of the pulse and to mitigation of its self-phase modulation. In the *strongly* nonlinear regenerator considered here, we observed qualitatively similar trends; however, we note that no rigorous theory of such a strongly nonlinear regime in the presence of dispersion management yet exists. In particular, changing the absolute value of map strength by the same amount for a regenerator and for a DM-soliton system may lead to qualitatively different changes in the behaviors of the corresponding pulses. Therefore, we use S merely as a label, referring to different regenerators by their map strengths relative to one another.

The loss of the HNLF and the PGDDs is ignored in this and the next Sections. This is done to have a direct comparison between current results and the results of Ref. [5]. In Section 4, we present results where the losses are taken into account. We also do not consider amplified spontaneous emission. While the signal-noise interaction in this strongly nonlinear system may be nonnegligible, its analysis is outside the scope of this work and is left for future research.

Since in most previous studies (except [5, 18]), the input-output power transfer curves were reported only for CD regenerators, we will first compare such curves for three cases: (a) a CD regenerator, (b) a DM regenerator with the parameters similar to those reported in [5, 18], and (c) another DM regenerator whose dispersion map is twice as strong. The former and latter DM regenerators have sixteen 0.5-km and eight 1-km HNLF sections, respectively, so that their total lengths both equal 8 km. According to Eq. (2), the regenerator in case (c) has a stronger dispersion map than that in case (b). In the CD regenerator, whose length is also 8 km, the dispersion of the HNLF coincides with the average dispersion. (The map strength of a CD regenerator is zero.) For the purpose of this comparison of CD and DM regenerators, PGDDs in the DM regenerators are assumed to have a constant amplitude characteristic (i.e., perform no filtering). The results are shown in Fig. 2, where the solid and dashed lines denote, respectively, the maximum and minimum powers of the regenerated ONEs. These powers are different mainly

because adjacent pulses interact due to their dispersion-induced spreading within each cell. As a result, ONEs that are in the middle of a group, those at a group's edges, and isolated ONEs, evolve differently. Note that some small difference between these curves (in what follows referred to as max-ONE and min-ONE curves) exists even in a CD regenerator due to the slight patterning effect of the input signal. A comparison of the three regenerators in Fig. 2 reveals two trends. First, with the increase of the dispersion map strength, the "dips" in the power transfer curves smoothen out. Second, as expected, the adjacent pulse interaction increases with the map strength, as manifested by the relative divergence of the min-ONE and max-ONE curves in Fig. 2(c) and also in Fig. 2(b) for $D_{av} = -8$ ps/nm/km.

Using these results, we will now give two criteria for a single-channel power transfer curve that would indicate whether a given regenerator can provide significant "clean-up" of both ZERO (poor extinction ratio) and ONE (amplitude jitter) levels. The first criterion is well known from the studies of a CD regenerator (see, e.g., [20] and references therein): the curve must
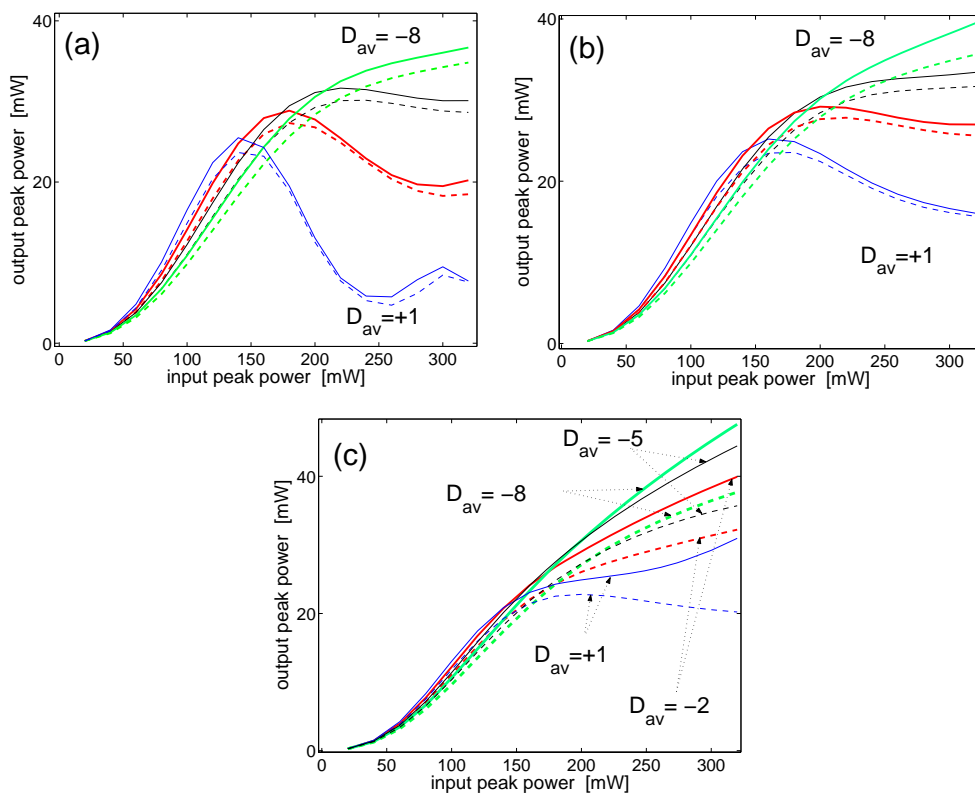

Fig. 2. Input-output power transfer curves of the CD (a) and DM (b,c) regenerators of the same total length of 8 km. In the DM cases, the PGDDs have a constant amplitude characteristic (i.e., no filtering), and HNLF consists of (b) 16×0.5-km and (c) 8×1-km sections. The other parameters are listed in the text. Note that according to Eq. (2), the dispersion map strengths increase from $S = 0$ (case (a)) to $S = 0.15$ (case (b)) to $S = 0.30$ (case (c)). In all figures, the average dispersions are, from top to bottom, -8, -5, -2, and $+1$ ps/nm/km. Within each figure, solid and dashed lines of the same color represent, respectively, the maximum and minimum powers of the regenerated ONEs for the same average dispersion.

have a concave upward region for small powers (with near-zero derivative at zero power) and a plateau for large ones. Second, the min-ONE and max-ONE curves must be close to one another. Quantitatively, they should be about as close as they are for a CD regenerator. This second condition is specific to DM regenerators. Using these two criteria, we conclude from Figs. 2(b,c) that a "good" regenerator in this figure is the one in panel (b) (i.e., that with the smaller map strength) for the average dispersion between -5 and -2 ps/nm/km. For other values of D_{av}, the plateau in the curves disappears. Also, for the regenerator with the stronger map (Fig. 2(c)), the min-ONE and max-ONE curves diverge from each other. In both of these cases, the amplitude jitter of ONEs will not be cleaned by such a regenerator.
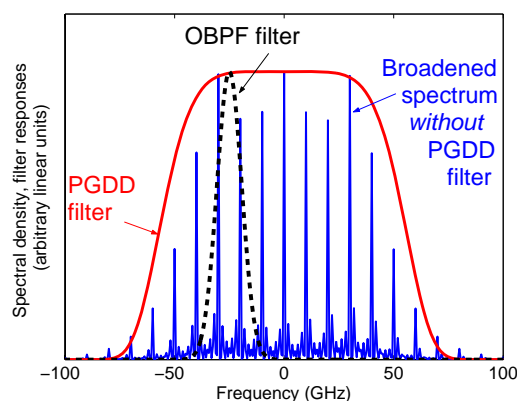

Fig. 3. Blue line: Spectral density of the broadened pulses at the output of the DM regenerator shown in Fig. 2(b) with $D_{av} = -4$ ps/nm/km and input peak power of 280 mW. Red solid and black dashed lines: (squared) amplitude responses of modeled PGDD and OBPF. Note that since a regenerator contains several PGDDs, the wings (extending beyond 30 GHz from the channel center) of the signal spectrum in in the presence of PGDD's amplitude response would be filtered stronger than it may appear from the response of a single PGDD shown above.

Next, in Fig. 4 we show the power transfer curves for the same DM regenerators as in Figs. 2(b,c), but where the PGDDs have the amplitude characteristic of a 110-GHz-wide 3rd-order Gaussian, emulating that of the commercial PGDD used in one of the authors' (M.V.'s) lab. This characteristic in relation to the broadened pulse spectrum and the location of the OBPF in the frequency domain is shown in Fig. 3. It is seen from Fig. 4 that the introduction of such filtering by PGDDs destroys the plateau of a transfer curve. Thus, the regenerator with a realistic PGDD will not be able to operate successfully in the regime we originally found in [5, 18]. Therefore, we looked for another regime where transfer curves would have plateaus and the min-ONE and max-ONE curves would be sufficiently close to one another in the presence of filtering by PGDDs. The direction for our search was suggested by the results presented in Figs. 2 and 4, as we now explain. First, the reason why the regenerator with the weaker dispersion map is affected more by the PGDD filtering may be simply that it contains twice as many of these devices (since it has twice as many cells) as the other DM regenerator. Next, notice from Fig. 4(b) that the case with the *positive* D_{av} meets one of the two criteria stated above for a "good" regenerator: the corresponding min-ONE and max-ONE curves are close to one another. However, there is still no plateau in this case: the curves have a substantial negative slope. To remedy this problem, we recall from our discussion of Fig. 2 that the curves tend to flatten out when the map strength is increased. These observations led us to the finding of a new regime suitable for the regeneration when the PGDDs have a filtering amplitude characteristic.
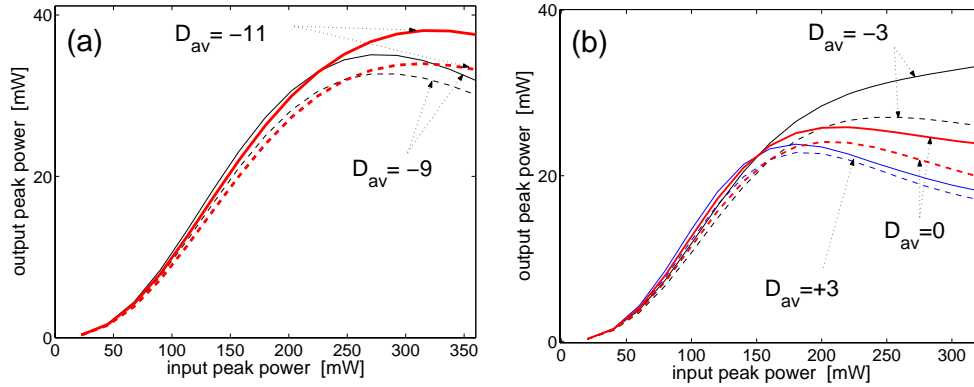
Fig. 4. Input-output power transfer curves of the DM regenerators similar to those shown in Fig. 2(b) (panel (a)) and Fig. 2(c) (panel (b)), except that the PGDDs now have an amplitude characteristic of a 110-GHz-wide 3rd-order Gaussian. Within each figure, solid and dashed lines of the same color represent, respectively, the maximum and minimum powers of the regenerated ONEs for the same average dispersion. Only the few "best" curves for each case are shown. The average dispersion values are quoted in units of ps/nm/km. Note that in (a), the range of the input powers in slightly increased compared to Fig. 2 to better show the details of the curves.

This new regime corresponds to a stronger dispersion map requiring fewer cells than before and also *large* and *positive* values of the average dispersion. Figure 5(a) shows the main result of this section: power transfer curves for a regenerator containing six cells with 1.25-km HNLF sections and the average dispersions of 10, 20, and 30 ps/nm/km. (For $D_{av} = 5$ ps/nm/km, the min-ONE and max-ONE curves are somewhat further apart than for the cases shown, and hence are not displayed.) This figure shows that not only do plateaus of proximate min-ONE and max-ONE curves exist in this regime, but they also do so for a much wider range of average dispersion values than in the regime reported in Fig. 2. As a side note, we point out that this regime is qualitatively different from that of soliton-like compression (see, e.g., [4]). Indeed, the pulse spectrum in this regime is broadened by a factor of several times (otherwise spectrum slicing by an OBPF would not be successful), while in the soliton-like compression, the spectrum broadening is less than by a factor of two.

We verified that in addition to being robust to variations of the value of D_{av}, this new regime is also robust with respect to the following factors: (i) chirp of the input pulses, between 0 and +100 ps/nm; (ii) postcompensation after the regenerator, between 0 and −100 ps/nm; (iii) fluctuations of values of D_{av} in individual cells by up to 100% as long as the average dispersion of the entire regenerator is in the range between 10 and 20 ps/nm/km; (iv) small (up to 10 GHz) shifts of the PGDDs central wavelength relative to the channel center; see Fig. 5(b). (We also verified that if, in the new regime, the PGDDs have a constant amplitude characteristic, i.e. provide no filtering, the shapes of the transfer curves do not differ significantly from the corresponding shapes in Fig. 5.) Moreover, we found that a regenerator with seven or five such cells performs similarly to the one with six cells, the main difference being in the power at which the plateau of the curves is formed; see Fig. 5(c). Such a remarkable robustness of the new regime obviates the need for a very precise tuning of both the input pulse parameters and the parameters of the regenerator. Last but not least, this new regime requires much fewer cells, and hence much fewer PGDDs, than the previously reported regime. This results in saving on the cost of the PGDDs and also the amplifiers that are required to compensate for the insertion loss of the PGDDs (about 2 dB per commercially available device) plus the loss of the HNLF
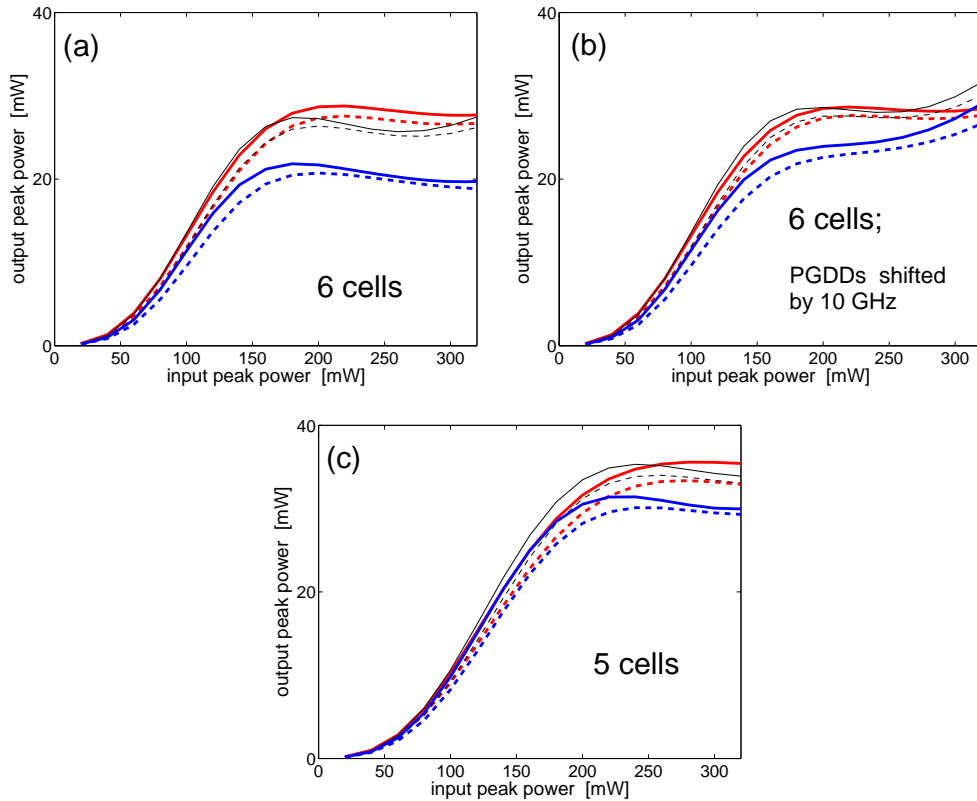
Fig. 5. Input-output power transfer curves of the DM regenerator in the new regime. The PGDDs have an amplitude characteristic of a 110-GHz-wide 3rd-order Gaussian, as in Fig. 4; in panel (b), the central frequencies of all the PGDDs are shifted by 10 GHz from the channel's center. The numbers of cells with 1.25-km HNLF sections are as indicated in the plots. The average dispersions are, from top to bottom, +10, +20 (thinner curves), and +30 ps/nm/km. Within each figure, solid and dashed lines of the same color represent, respectively, the maximum and minimum powers of the regenerated ONEs for the same average dispersion.

(about 4 dB for the entire 8-km length).

3. Multichannel results for the lossless case

We now demonstrate that a regenerator operating in the new regime improves the quality of a degraded signal in the WDM case. In our simulations, five co-polarized channels are spaced 200 GHz apart. In a typical 50-GHz-spaced WDM system, this can be achieved by using a standard 1:4 de-interleaver at the regenerator input, which separates the incoming channels into four sets with a four-time greater channel spacing. As noted in [18], the de-interleaver can either be a part of the regenerator (for a stand-alone regenerator) or be external to it (e.g. if the regenerator is co-located with an optical add-drop-multiplexer node commonly employing such de-interleavers [21]). The channels contain an identical but randomly time-shifted $(2^7 - 1)$-long pseudo-random bit sequence. We simulate seven different sets of interchannel bit delays, and below report results for the worst channel in the worst-performing of these sets. The degra-

dation of ZEROs is modeled by a low extinction ratio (8 dB) and the degradation of ONEs is modeled by a high amplitude jitter (60% peak-to-peak); these numbers are the same as in [5] so as to provide a direct comparison between our results in these two studies. Figure 6 shows eye diagrams for a regenerator with the parameters reported in Fig. 5(a) and $D_{av} = 15$ ps/nm/km. The average input peak power of ONEs is 235 mW. As a benchmark for multichannel simulations, we show, in panel (b), a single-channel output of such a regenerator. As was noted in [1], the amplitude jitter of the input pulses is transformed by the regenerator into their timing jitter. The net result is still a significant (2.1 dB) improvement of the eye opening. Panels (c) through (e) show the worst channel of a five-channel output. The values of the eye opening compared to the input are listed in the figure caption, where, as in [5], the eye opening is measured with a 10-ps "window" and the average peak powers of the input and output are rescaled to be the same.

Panel (c) is for the output with all the parameters as described above and for the OBPF offset from the channel's center by 25 GHz, as in all the simulations reported so far. The eye opening improvement in this case is 1.0 dB. To confirm the robustness of this new regime, we verified that the variations of the four factors listed at the end of the previous section do not degrade the eye opening by more than 0.2 dB, and neither do fluctuations of the average input power by 10% and of the OBPF's central frequency by at least 2.5 GHz. For example, panel (d) shows the output signal in the same case as in (c) except that the OBPF was offset from the channel's center by 20 GHz. Moreover, further optimization is possible with respect to some of these parameters. For example, panel (e) shows a net 1.4-dB eye opening improvement when the PGDDs in all cells are shifted by 20 GHz from the channel's center (in the same direction in which the OBPF at the regenerator output is offset). Furthermore, an additional slight but consistent (i.e. observed for all sets of interchannel bit delays) eye opening improvement by 0.1 dB is gained when the amplitude characteristic of the PGDDs is narrowed to 90 GHz and the input power is increased to 260 mW. (Note that such PGDDs are also easier to manufacture than the 110-GHz wide ones.) We also verified that a regenerator consisting of five (instead of six) cells exhibits similar performance, provided the input power is increased by about 15–20%. Thus, Fig. 6, which contains the main results of this section, demonstrates that not only the regenerator in the new regime exhibits a significantly better performance than in the regime originally proposed in [5], but also that this new regime exists over a relatively wide range of parameters.

Finally, in [5] we demonstrated that if in the previous regime, the PGDDs were replaced by conventional fiber dispersion-compensating modules (DCMs), which have a monotonic rather than periodic group delay function, the regeneration completely failed. Surprisingly, this is not so for the new regime. Figure 6(f) shows the output signal for the case where all PGDDs are replaced with fiber DCMs, with the remaining parameters being the same as in Fig. 6(c). Although the resulting timing and amplitude jitters are rather high, there is still a small improvement of the eye opening. The reason why the pulse quality is not degraded now nearly as much as it was in a similar situation considered in [5], is the high value of the average dispersion. It makes two overlapping bits in adjacent channels completely separate after just two regenerator cells, and hence the timing jitter is diminished compared to that in the regime with the smaller D_{av} reported in [5]. We emphasize, however, that the use of PGDDs instead of fiber DCMs improves the eye opening by more than an additional 1 dB. Thus, a PGDD is still a key element of the multichannel regenerator. Moreover, using fiber DCMs instead of PGDDs is, at least at this time, *not* a practical solution because there exist no commercially available single-mode fiber with anomalous dispersion matching or exceeding that of the HNLF quoted above. Note that using the standard single-mode fiber instead would result not only in significant loss and bulkiness of the device, but also in nonnegligible nonlinearity of the anomalous-dispersion

fiber sections, whose effect on the regeneration would not be obvious.

4. Results for cases with periodically compensated losses

The main sources of power loss in the DM regenerator are PGDDs: current commercially available samples have insertion loss of 2–3 dB. Compensating for these losses by placing an amplifier after every cell does not appear to be practical. Therefore, below we consider two cases where the losses of PGDDs and HNLF sections are compensated after every second or every third cell. Then, the 6-cell regenerator considered above will require only two or one amplifier in addition to that at the regenerator's input.

In the simulations reported below, we assumed the loss of a single PGDD to be 2.5 dB and the loss of the HNLF to be 0.5 dB/km. All the other details of the single- and five-channel simulations are the same as in Sections 2 and 3. Figures 7(a,b) show the power transfer curves analogous to those shown in Fig. 5(a), except that the losses are compensated after every second and every third cell, respectively. (The reason why the output powers are different from each other and from those in Fig. 5(a) is that in our simulations, the loss compensation at the regenerator's last cell brings up the average output power (before the OBPF) to its level at the input. This convention has no effect on the regenerator's performance.) It is seen that the account of periodically compensated losses does not significantly affect the single-channel results, except that the input power is to be greater than in the lossless case. The results for five-channel simulations are obtained in the same three cases as considered in Section 3: (i) all PGDDs are 110-GHz wide and not shifted relative to the channels' centers (to be compared with the results of Fig. 6(c)); (ii) the same PGDDs are shifted by 20 GHz relative to the channels (to be compared with the results of Fig. 6(e)); and (iii) the PGDDs are 90-GHz wide and shifted by 20 GHz (to be compared with the 0.1-dB improvement over the results of Fig. 6(e)). When the losses are compensated after every second cell and the input peak power per channel is 400 mW, the eye opening improvements (quoted, as before, for the worst channel of the worst-case set of interchannel bit delays) are 1.0, 1.3, and 1.4 dB, respectively. When the losses are compensated after the third cell and the input peak power is 500 mW, those improvements are 0.5, 1.0, and 1.1 dB.

The observed degradation of the regenerator's performance compared with that in the lossless case is analogous to a similar phenomenon of increased timing jitter in soliton transmission systems with periodically compensated losses [22]. Namely, in the presence of losses, the frequency shift occuring at the beginning of the collision of a given pulse with a pulse in another channel is not completely undone during the end of the same collision. This leads to residual collision-induced frequency shifts, which are translated, due to a nonzero average dispersion, into position shifts (i.e., timing jitter) of the pulses. Some mitigation of this signal degradation may be possible by optimizing such parameters as the input power, the amount of loss compensation inside the regenerator, average dispersion and the map strength, and dispersion precompensation. For example, for the aforementioned case (ii) where 110-GHz-wide PGDDs are shifted by 20 GHz relative to the channels and losses are compensated after the third cell, using a precompensation of $+100$ ps/nm (instead of the quoted earlier 0 ps/nm) followed by a postcompensation of -100 ps/nm, improves the worst-case eye opening by an additional 0.1 dB. We did not undertake a careful optimization of the regenerator's performance because this is not a goal of this paper. Rather, we emphasize that even in the presence of losses, the multichannel regenerator can provide eye-opening improvement between 1 and 1.5 dB (depending on the details of loss compensation) *without precise tuning* of its parameters.

We now briefly comment on the amount of amplified spontaneous emission noise that the amplifiers compensating for the losses inside the regenerator would produce. Due to relatively low gain (about 7–9 dB per such an amplifier), that amount is small compared to the amount

of noise produced by the high-gain amplifier at the regenerator's input, which needs to boost the signal's peak power from a few milliwatts to several hundreds of milliwatts. Moreover, even this latter amount degrades the signal-to-noise ratio much less than the noise added by an amplifier at the end of a single transmission span in a long-haul system (because in that case, the signal is being amplified from about a 0.01 mW to a few milliwatts). Thus, the total amount of noise added at the regenerator contributes very little to the overall degradation of the signal at its input.

5. Conclusions

In this work, we have demonstrated that the presence of an amplitude characteristic (i.e., filtering) of commercially available PGDDs destroys the capabilities of a multichannel 2R regenerator in the regime reported in Ref. [5]. We have found a new regime in which the regenerator's performance is robust not only to such filtering but also to considerable variations of the regenerator parameters. Moreover, such a regenerator requires fewer PGDDs (6 or 5 versus 16) than that reported in [5]. These factors have the potential to lead to a significant reduction of cost and complexity of a multichannel regenerator. We also point out that a DM regenerator has more optimization parameters than a CD regenerator, which may leave room for further optimization of its performance. Interestingly, a finite-width amplitude characteristic of the PGDDs, which was a detrimental factor for the original regeneration regime, can be used as one of the optimization parameters in the new regime. The maximum improvement in eye opening that we have obtained in this paper is 1.5 dB for the lossless regenerator and 1.4 dB for a regenerator where the losses of PGDDs and HNLF are compensated after every two cells.
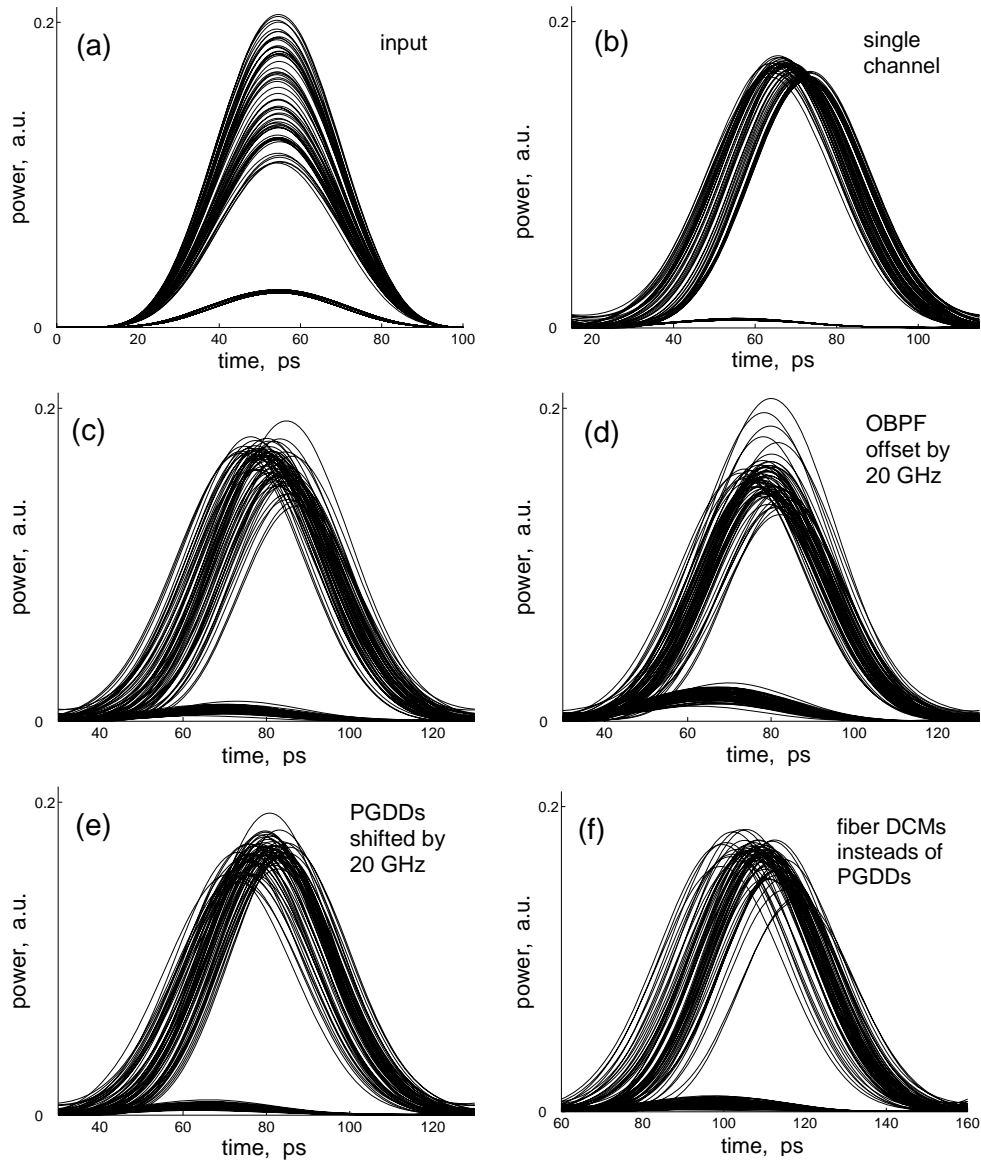
Acknowledgement

Fig. 6. Eye diagrams for a regenerator with six 1.25-km cells and $D_{av} = 15$ ps/nm/km. The input signal has the average peak power of 235 mW. Panel (a) shows the input signal and panel (b) shows the output of a single-channel regenerator. Panels (c)–(f) show the worst channel for the five-channel output. The PGDDs are 110 GHz wide for (b)–(e) and centered at the channels for (b)–(d) and shifted from them by 20 GHz for (e). Panel (f) corresponds to the case where all PGDDs are replaced by fiber DCMs. All outputs (b) – (f) except (d) are obtained with the OBPF offset by 25 GHz from the channel's center; in (d), the OBPF is offset by 20 GHz. The eye-opening improvements over the input (a) are, in dB: 2.1 (b), 1.0 (c), 0.9 (d), 1.4 (e), 0.3 (f).
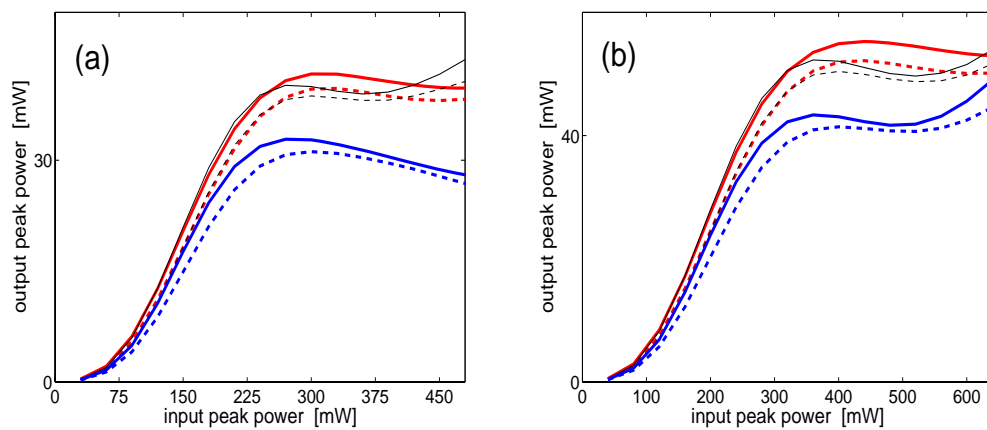
Fig. 7. Same as in Fig. 5(a), but the PGDD and HNLF losses are taken into account and are compensated after every second (a) and third (b) cells.